

## RESEARCH OUTPUTS / RÉSULTATS DE RECHERCHE

### Temperature and dose dependences of nitrogen implantation into iron

Terwagne, Guy; Bodart, Franz; M. Piette, [No Value]; P. Bertrand, [No Value]

*Published in:*

Materials Science and Engineering

*Publication date:*

1989

*Document Version*

Early version, also known as pre-print

[Link to publication](#)

*Citation for pulished version (HARVARD):*

Terwagne, G, Bodart, F, M. Piette, NV & P. Bertrand, NV 1989, 'Temperature and dose dependences of nitrogen implantation into iron' Materials Science and Engineering, vol. B2, pp. 195-201.

#### General rights

Copyright and moral rights for the publications made accessible in the public portal are retained by the authors and/or other copyright owners and it is a condition of accessing publications that users recognise and abide by the legal requirements associated with these rights.

- Users may download and print one copy of any publication from the public portal for the purpose of private study or research.
- You may not further distribute the material or use it for any profit-making activity or commercial gain
- You may freely distribute the URL identifying the publication in the public portal ?

#### Take down policy

If you believe that this document breaches copyright please contact us providing details, and we will remove access to the work immediately and investigate your claim.

## Temperature and Dose Dependences of Nitrogen Implantation into Iron\*

G. TERWAGNE and M. PIETTE

Laboratoire d'Analyses par Réactions Nucléaires, and Institute for Studies in Interface Sciences, Facultés Universitaires N.-D. De la Paix, B-5000 Namur (Belgium)

P. BERTRAND

Laboratoire de Physico-Chimie et de Physique des Matériaux, Université Catholique de Louvain, Louvain-la-Neuve (Belgium)

F. BODART

Laboratoire d'Analyses par Réactions Nucléaires, and Institute for Studies in Interface Sciences, Facultés Universitaires N.-D. De la Paix, B-5000 Namur (Belgium)

(Received June 2, 1988)

### Abstract

It has been shown that the depth profile of nitrogen implanted into iron depends strongly on the temperature during and after the implantation. The nitrogen depth profile shows a surface peak which increases with increasing implantation temperature. A systematic study of nitrogen-implanted iron has been performed with different experimental techniques in order to explain this temperature effect.

Pure iron samples have been implanted with 100 keV  $^{15}\text{N}_2^+$  ions at different doses ( $5 \times 10^{16}$ – $5 \times 10^{17}$  ions  $\text{cm}^{-2}$ ) and at various temperatures (20–200 °C). The specimens were studied by conversion electron Mössbauer spectroscopy in order to measure the relative concentration of iron nitrides such as  $\epsilon\text{-Fe}_2\text{N}$ ,  $\epsilon\text{-Fe}_3\text{N}$  or  $\gamma'\text{-Fe}_4\text{N}$  formed after nitrogen implantation.

These results have been correlated with the nitrogen diffusion process deduced from the nuclear profile taken on the same specimens. The nitrogen surface peak was carefully examined by combining ion scattering spectrometry and secondary ion mass spectrometry with ion beam sputter profiling of the samples. The depth profile of nitrogen clearly shows that nitrogen diffuses towards the surface when the sample is heated during the implantation.

### 1. Introduction

Over the last decade, nitrogen implantation has been used, in some cases on an industrial scale, to enhance the friction wear and corrosion properties of steels and alloys. Despite considerable research effort by many workers whose aim was to elucidate the mechanism responsible for the modification of the chemical and mechanical properties which nitrogen implantation produces, our understanding of this phenomenon remains inadequate. Experimental work [1–4] has shown that the concentration profile of implanted nitrogen into steels varies very strongly with parameters such as flux, dose and substrate temperature during implantation. A study of nitrogen-implanted iron foils by conversion electron Mössbauer spectroscopy (CEMS) has been performed 10 years ago by Longworth and Hartley [5], but they seemed to ignore an important parameter—the sample temperature during the implantation. Nevertheless, this work is complete and shows the evolution of iron nitride when the implanted sample is annealed. The aim of the present work is to study the temperature and dose dependences of nitrogen implanted into iron by using different techniques; the iron nitride phase formed after implantation into iron was studied by CEMS, the nitrogen depth profile evolution was measured by nuclear reaction analysis (NRA) and the surface layer of the implanted iron was studied by combining ion scattering spectrometry (ISS) and secondary ion mass spectrometry (SIMS).

\*Paper presented at the Symposium on Ceramic Materials Research at the E-MRS Spring Meeting, Strasbourg, May 31–June 2, 1988.

## 2. Experimental procedure

### 2.1. Sample preparation

Polycrystalline pure iron discs of diameter 18 mm and thickness 0.25 mm were mechanically polished with diamond paste (15 and 1  $\mu\text{m}$ ) and then with alumina powder (1 and 0.05  $\mu\text{m}$ ). They were implanted with 100 keV  $^{15}\text{N}_2^+$  ions using the SAMES implanter in Namur. The vacuum in the implantation chamber was achieved using a turbopump; a cold trap was placed in the vicinity of the specimen in order to reduce the carbon contamination; this system gave a residual pressure of  $3 \times 10^{-7}$  Torr before the implantation and of  $2 \times 10^{-6}$  Torr during the implantation owing to the  $^{15}\text{N}$  residual gas coming from the ion source. The beam current density was generally of the order of  $5 \mu\text{A cm}^{-2}$ . A special sample holder allowed a specimen temperature of between  $-196$  and  $450^\circ\text{C}$  with a precision of  $5^\circ\text{C}$ . Rapid cooling of the target was performed after the implantation. The iron samples were implanted with a homogeneous dose of  $5 \times 10^{16}$ – $5 \times 10^{17}$  ions  $\text{cm}^{-2}$  at temperatures of  $20$ – $200^\circ\text{C}$ .

### 2.2. Depth profiling of $^{15}\text{N}$

The nitrogen distribution was measured using the nuclear resonant reaction  $^{15}\text{N}(p, \alpha\gamma)^{12}\text{C}$  at  $E_p = 429$  keV. The nitrogen depth profile was obtained with an automatic energy scan installed on a 2.5 MV Van de Graaff accelerator in Namur. The  $\gamma$ -rays were detected with a  $4 \text{ in} \times 4 \text{ in}$  NaI scintillator. The experimental data were deconvoluted in order to obtain the true nitrogen distribution. The deconvolution technique has been presented in a previous paper [4].

### 2.3. Conversion electron Mössbauer spectroscopy measurements

CEMS was used to determine the different phases formed after nitrogen implantation in the iron samples. The Mössbauer measurements were made using a  $^{57}\text{Co}$  source in a rhodium matrix with an activity of 50 mCi. The specimen of interest was placed in a gas flow proportional counter where 7.3 keV conversion electrons resulting from recoilless resonant absorption by  $^{57}\text{Fe}$  nuclei within the specimen were detected. The 5.6 keV Auger electrons emitted after the electronic rearrangement following the internal conversion were also detected. It has been shown experimentally [6] that the detection of 7.3 and 5.6 keV electrons results in 65% of the signal

coming from within a depth of 60 nm. The experimental Mössbauer spectra were deconvoluted and analysed by means of an interactive computer program which allowed adjustment of the various hyperfine parameters.

### 2.4. Surface spectrometries

The ISS and SIMS surface analyses were performed at Louvain using the same experimental system. The residual pressure in the analysis chamber was  $10^{-9}$  Torr and this rose to  $2 \times 10^{-7}$  Torr when the ion beam was on. The ISS spectrometer (Kratos WG 541) consists of a cylindrical mirror energy analyser with an integrated coaxial ion gun. In this configuration, the backscattering is performed at  $138^\circ$ . The SIMS spectrometer (Riber Q156) consists of a  $45^\circ$  deflection energy selector and a quadrupole mass filter. Detection was done at  $90^\circ$  with respect to the beam direction. Automatic sequences of analyses and sputter depth profiling were performed with a multichannel analyser (Lecroy MCA 3500). Typical working conditions for SIMS and ion beam sputter depth profiling were as follows. A 4 keV  $\text{Xe}^+$  ion beam with a current of 50 nA and a beam spot diameter of 200  $\mu\text{m}$  was rastered onto a square sample area of 1.8 mm side. A sputter velocity of about  $10^{-2} \text{ \AA s}^{-1}$  was obtained. The SIMS signal was only accepted when the beam was in the central part of the crater (9% of the total signal). To obtain the concentration depth profiles, the intensities at the maximum of the selected  $q/m$  peaks are accumulated for 10 s and stored as a function of the bombardment time. The depth calibration was done by measuring the crater shape with a profile meter (Sloan Dektak). For the ISS analyses, a 2 keV  $\text{He}^+$  ion beam of 10 nA at normal incidence to the surface was used.

## 3. Results

### 3.1. Nitrogen depth profile

Figure 1(a) shows the deconvoluted depth profile of nitrogen for a constant dose of  $2 \times 10^{17}$  ions  $\text{cm}^{-2}$  as a function of temperature (20, 80, 120, 160 and  $200^\circ\text{C}$ ). The depth concentration for the low implantation temperature ( $20^\circ\text{C}$ ) shows a gaussian shape with the maximum position at 62 nm and a width of 36 nm, which corresponds roughly to the predicted values for the projected range  $R_p$  and range straggling  $\Delta R_p$  calculated with the TRIDYN code [7] ( $R_p = 63$

nm;  $\Delta R_p = 26$  nm). At higher temperatures, a surface contribution appears which increases with the specimen temperature. This temperature effect has already been observed for nitrogen implantation in various steels [4, 8]. The total area under each nitrogen contribution is mainly constant. This means that the remaining amount of nitrogen does not decrease when the tempera-

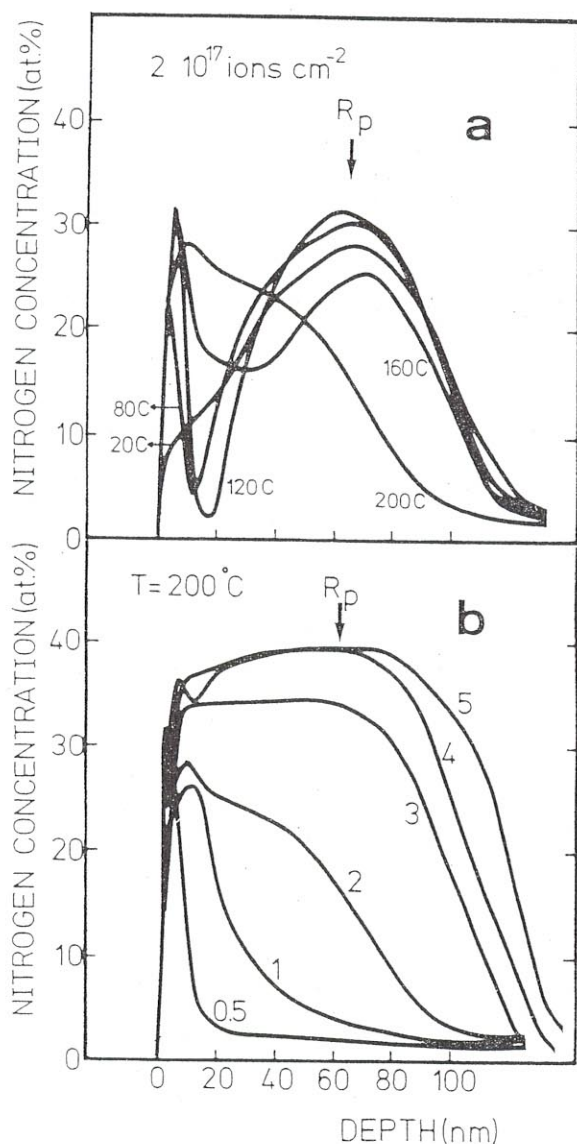


Fig. 1. (a) Deconvoluted depth profile for 100 keV  $N_2^+$  ions implanted into pure iron at a dose of  $2 \times 10^{17}$  ions  $cm^{-2}$  and at various temperatures (20, 80, 120, 160 and 200 °C).  $R_p$  indicates the projective range calculated by TRIDYN code. (b) Deconvoluted depth profile for 100 keV  $N_2^+$  ions implanted into pure iron at a constant temperature of 200 °C. The numbers indicated on the curves are the doses expressed in  $10^{17}$  ions  $cm^{-2}$ .

ture increases (at least until 200 °C), which means that nitrogen does not diffuse out of the sample.

Figure 1(b) shows the deconvoluted nitrogen distribution obtained on iron samples implanted at different doses ( $5 \times 10^{16}$ – $5 \times 10^{17}$  ions  $cm^{-2}$ ) at the same temperature (200 °C). We can observe that for lower doses ( $5 \times 10^{16}$ – $2 \times 10^{17}$  ions  $cm^{-2}$ ) the nitrogen distributions do not have a gaussian shape around  $R_p$  but there is a high concentration of nitrogen near the surface. The area of the surface peak increases with the dose up to saturation (about 35%); this means that nitrogen diffuses from the bulk to near the surface during the implantation. For higher doses ( $3 \times 10^{17}$ – $5 \times 10^{17}$  ions  $cm^{-2}$ ), the bulk contribution becomes increasingly more important and the shape of the distribution is rectangular. This is the saturation effect; there is no more than 40 at.% N in the implanted iron.

### 3.2. Conversion electron Mössbauer spectroscopy experiments

In order to obtain precise hyperfine parameters for the deconvolution of the Mössbauer spectra, we first measured the Mössbauer spectrum of an iron nitride powder (325 mesh) which contained  $Fe_2N$ ,  $Fe_3N$  and  $Fe_4N$  (Fig. 2); measurements using the X-ray powder diffraction technique showed that the major constituent of iron nitride is the  $\gamma'$ - $Fe_4N$  phase. We obtained a good fit of the iron nitride Mössbauer spectrum if we introduced the hyperfine parameters taken from the literature for  $\epsilon$ - $Fe_2N$  [9] and  $\epsilon$ - $Fe_3N$  [10] and the hyperfine parameters for  $\gamma'$ - $Fe_4N$  calculated

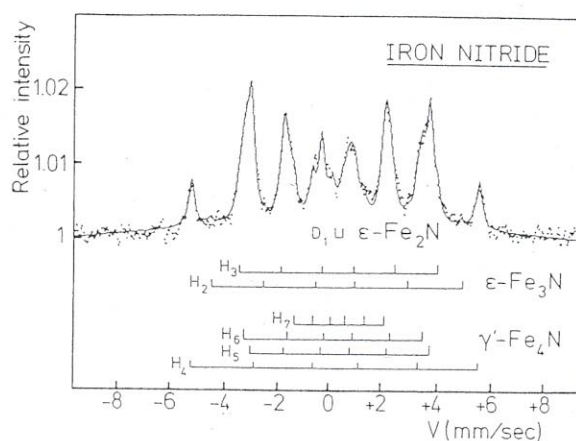


Fig. 2. Mössbauer spectrum of an iron nitride powder (325 mesh) which contains:  $\epsilon$ - $Fe_2N$ ,  $\epsilon$ - $Fe_3N$  and  $\gamma'$ - $Fe_4N$ . The curve was obtained by adjusting the experimental data with the parameters in Table 1.

from Fig. 1 of Nozik's paper [11]; the hyperfine parameters in Table 1 of Nozik's paper do not agree with the Mössbauer spectrum in Fig. 1 of Nozik's paper. The results from our calculation are reported in Table 1. The width of all components are the same and fixed at  $0.29 \text{ mm s}^{-1}$ . The quadrupole splittings for  $H_5$  and  $H_6$  are respectively  $+0.26$  and  $-0.45 \text{ mm s}^{-1}$  in place of  $-0.22$  and  $0.43 \text{ mm s}^{-1}$  and the isomer shifts for  $H_5$  and  $H_6$  (with respect to iron) are  $0.31$  and  $0.25 \text{ mm s}^{-1}$  in place of  $+0.52$  and  $-0.15 \text{ mm s}^{-1}$ , which are the hyperfine parameters from ref. 11. Furthermore, the theoretical fit is in agreement with the experimental data if we insert a supplementary sextuplet denoted  $H_7$  in Fig. 2. We have attributed this last component to the  $\gamma'$ - $\text{Fe}_4\text{N}$  structure. We shall take the hyperfine parameters from Table 1 and hyperfine parameters for  $\alpha$ -Fe in order to fit the Mössbauer spectra obtained for the implanted specimens.

The Mössbauer spectra obtained for iron samples implanted at  $200^\circ\text{C}$  with different doses ( $5 \times 10^{16}$ – $5 \times 10^{17} \text{ ions cm}^{-2}$ ) are presented in Fig. 3. For the lower doses ( $5 \times 10^{16}$ – $2 \times 10^{17} \text{ ions cm}^{-2}$ ) the  $\alpha$ -Fe phase decreases when the dose increases. At a dose of  $2 \times 10^{17} \text{ ions cm}^{-2}$ , it can be seen in Fig. 4 that the  $\gamma'$ - $\text{Fe}_4\text{N}$  phase is well defined. For doses below saturation ( $3 \times 10^{17} \text{ ions cm}^{-2}$ ), the  $\alpha$ -Fe phase is transformed into  $\gamma'$ - $\text{Fe}_4\text{N}$  and  $\epsilon$ - $\text{Fe}_3\text{N}$ . At higher doses ( $3 \times 10^{17}$ – $5 \times 10^{17} \text{ ions cm}^{-2}$ ), we can observe a double peak denoted  $D_1$  in the Mössbauer spectra; this is due to the  $\epsilon$ - $\text{Fe}_2\text{N}$  phase which appears at doses between  $2 \times 10^{17}$  and  $3 \times 10^{17} \text{ ions cm}^{-2}$  (Fig. 4). The concentration of  $\alpha$ -Fe phase is still constant between  $3 \times 10^{17}$  and  $5 \times 10^{17} \text{ ions cm}^{-2}$ . This means that the saturation

dose for  $50 \text{ keV}$  nitrogen implanted into iron is reached at  $3 \times 10^{17} \text{ ions cm}^{-2}$ .

Mössbauer spectra have been measured from iron samples implanted with the same dose ( $2 \times 10^{17} \text{ ions cm}^{-2}$ ) but at different temperatures ( $20, 80, 120, 160$  and  $200^\circ\text{C}$ ). The results of the deconvoluted experimental data are presented in Fig. 5 which shows the relative concentrations of the different phases in the implanted specimens for various temperatures. The concentration of the  $\alpha$ -Fe phase slowly increases with increasing temperature while the concentration of  $\epsilon$ - $\text{Fe}_3\text{N}$  phase linearly decreases. Finally, the concentration of the  $\gamma'$ - $\text{Fe}_4\text{N}$  phase shows a large variation for the different implantation temperatures.

### 3.3. Ion scattering spectrometry and secondary ion mass spectrometry

Implanted and pure iron samples show the same SIMS mass spectra measured up to  $q/m = 150$ , except for intensities associated with  $^{15}\text{N}$ ,  $\text{Fe}^{15}\text{N}$  and  $\text{Fe}_2^{15}\text{N}$ . Also the oxygen intensity is higher in the implanted sample. The spectra reflect sample composition, surface contamination and surface treatment. SIMS  $^{15}\text{N}$  depth profiles are in good agreement with those obtained by nuclear methods. Figure 6(a) shows the result for a sample implanted at  $50 \text{ keV}$  with  $2 \times 10^{17} \text{ ions cm}^{-2}$  and heat treated at  $120^\circ\text{C}$  during implantation. A surface peak is also noted, which is compared with the carbon and oxygen profiles in Fig. 6(b). It should be noted that these profiles are not correlated. The first rapid  $15 \text{ amu}$  signal decrease observed at the beginning of bombardment corresponds to the sputtering of  $\text{CH}_3$  originating from a surface hydrocarbon contamination layer.

TABLE 1 Hyperfine parameters obtained after the deconvolution of the iron nitride Mössbauer spectrum in Fig. 2

Component	$H$ (kOe)	Isomer shift <sup>a</sup> ( $\text{mm s}^{-1}$ )	Quadrupole splitting ( $\text{mm s}^{-1}$ )	Relative area (%)	Phase
$D_1$	—	0.37 (0.03)	0.34 (0.04)	3.6 (0.4)	$\epsilon$ - $\text{Fe}_2\text{N}$
$H_2$	297 (4)	0.239 (0.005)	—	2.0 (1.0)	$\epsilon$ - $\text{Fe}_3\text{N}$
$H_3$	236 (2)	0.330 (0.005)	—	5.2 (1.6)	$\epsilon$ - $\text{Fe}_3\text{N}$
$H_4$	337.8 (0.7)	0.23 (0.01)	—	17.1 (1.1)	$\gamma'$ - $\text{Fe}_4\text{N}$
$H_5$	214.7 (0.4)	0.314 (0.005)	0.26 (0.02)	37.5 (1.7)	$\gamma'$ - $\text{Fe}_4\text{N}$
$H_6$	212.7 (0.8)	0.253 (0.009)	0.45 (0.04)	20.3 (1.7)	$\gamma'$ - $\text{Fe}_4\text{N}$
$H_7$	110 (1)	0.37 (0.01)	—	13.4 (1.3)	$\gamma'$ - $\text{Fe}_4\text{N}$

The numbers indicated inside parentheses are the absolute errors.

<sup>a</sup>With respect to  $\alpha$ -Fe.

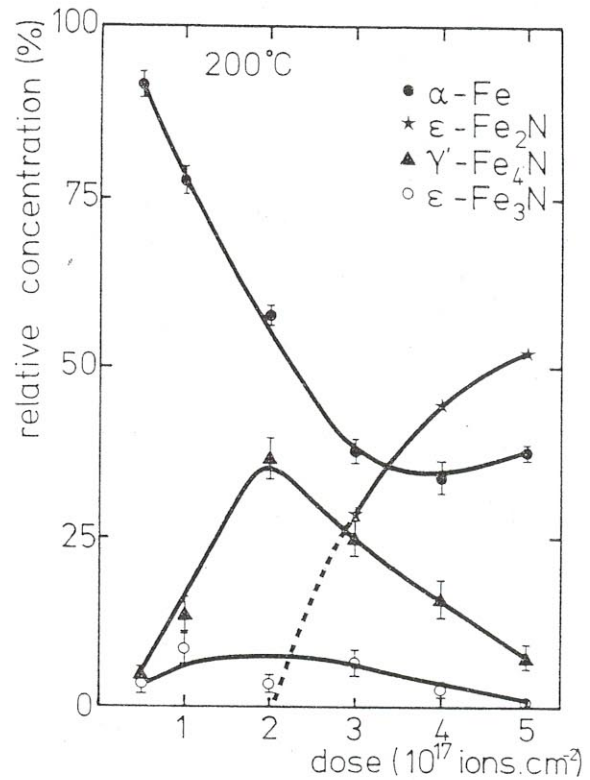
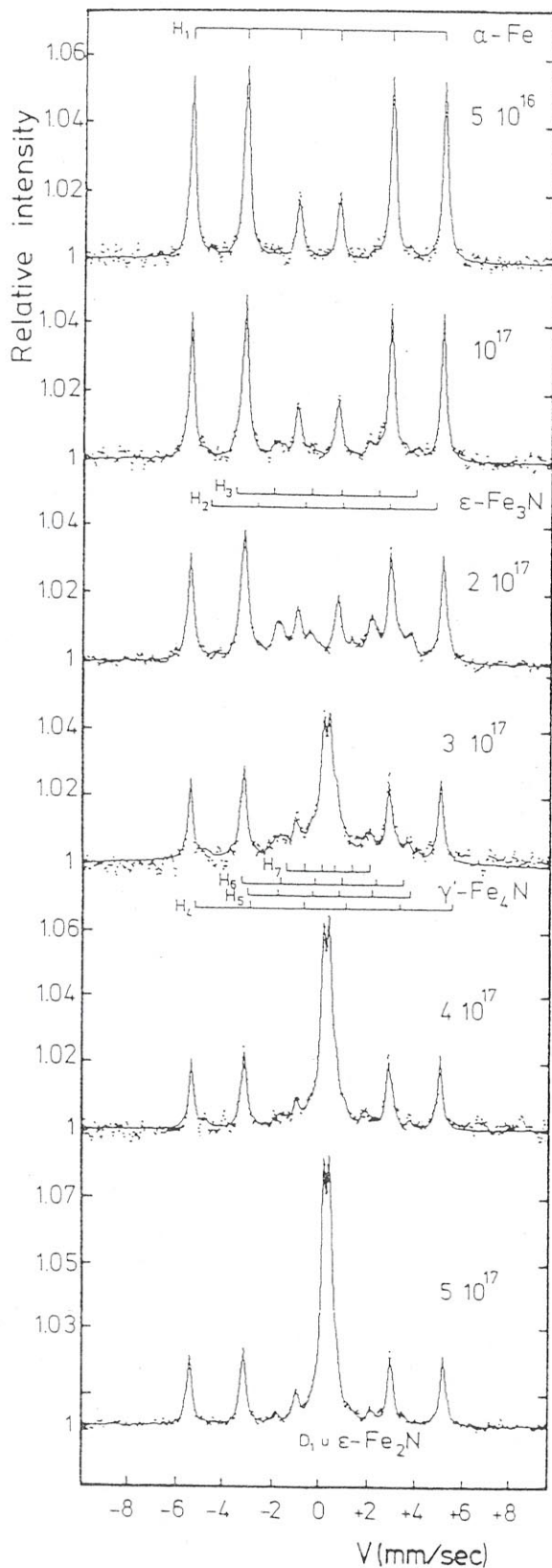


Fig. 4. Analysis of Mössbauer spectra showing the relative concentration of the different iron nitride phases formed after nitrogen implantation into pure iron at 200 °C and with different doses ( $5 \times 10^{16}$ – $5 \times 10^{17}$  ions  $\text{cm}^{-2}$ ).

ISS results also indicate a  $^{15}\text{N}$  contribution in the spectra for the implanted samples. However, owing to poor mass resolution, this contribution appears as a low energy shoulder in the oxygen peak and a peak decomposition is required to obtain the profiles. Nevertheless, the same double peak profiles are obtained for  $^{15}\text{N}$ .

#### 4. Discussion

Analysis of Mössbauer spectra for the implanted iron at 200 °C leads to the conclusion that iron nitrides are formed when the dose of nitrogen ions is greater than  $5 \times 10^{16}$  ions  $\text{cm}^{-2}$ . As the dose is increased above this value,  $\gamma'$ - $\text{Fe}_4\text{N}$  and a small amount of  $\epsilon$ - $\text{Fe}_3\text{N}$  are first formed, followed by a  $\epsilon$ - $\text{Fe}_2\text{N}$  phase formation when the saturation dose is reached ( $3 \times 10^{17}$  ions  $\text{cm}^{-2}$ ). For doses higher than the saturation dose,  $\gamma'$ -

Fig. 3. The Mössbauer electron scattering spectra at room temperature of a pure iron foil implanted at 200 °C with 100 keV  $\text{N}_2^+$  ions at different doses ( $5 \times 10^{16}$ – $5 \times 10^{17}$  ions  $\text{cm}^{-2}$ ).

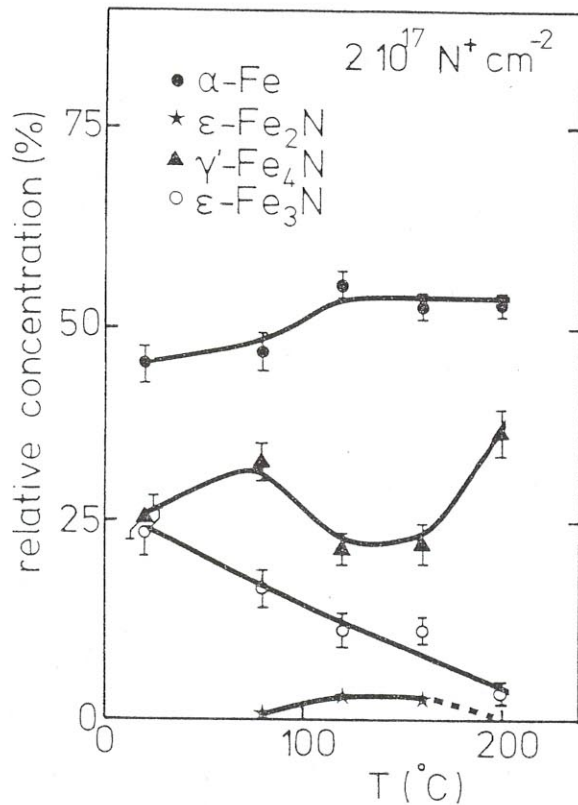


Fig. 5. Analysis of Mössbauer spectra showing the relative concentration of the different iron nitride phases formed after nitrogen implantation into pure iron with a constant dose ( $2 \times 10^{17}$  ions  $\text{cm}^{-2}$ ) at different temperatures.

$\text{Fe}_4\text{N}$  and  $\epsilon\text{-Fe}_3\text{N}$  are transformed into the  $\epsilon\text{-Fe}_2\text{N}$  phase which contains 33 at.% N; it is the most compact iron nitride which can be formed. A nitrogen concentration of 40 at.% is observed for doses higher than the saturation dose. This difference of 7 at.% can be explained by free nitrogen which is probably concentrated at the grain boundaries. It cannot be due to the formation of iron nitride because  $\alpha\text{-Fe}$  concentration remains constant above saturation.

Nitrogen distributions for high temperature implantation show that nitrogen diffuses towards the surface. This diffusion process leads to the formation of a surface peak which can be explained by the trapping of nitrogen into precipitation sites [12]. From the SIMS results, the implanted nitrogen seems to be bound only to iron;  $\text{FeN}$  and  $\text{Fe}_2\text{N}$  molecular ions are detected, but no  $\text{FeCN}$  compounds. Moreover the carbon profile is not correlated with that of nitrogen. The oxide surface layer detected by the SIMS technique appears to act as a diffusion barrier, preventing nitrogen migration to the extreme surface.

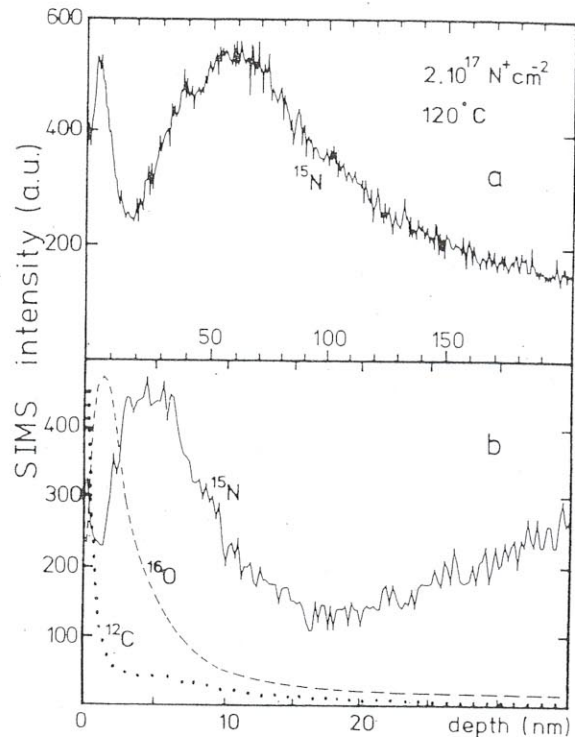


Fig. 6. (a) Nitrogen depth profile obtained by using the SIMS technique on a pure iron sample implanted with  $2 \times 10^{17}$  ions  $\text{cm}^{-2}$  at  $120^\circ\text{C}$  showing the existence of the surface peak at 5 nm below the surface; (b) SIMS profile of the first 30 nm on a pure iron sample implanted with  $2 \times 10^{17}$  ions  $\text{cm}^{-2}$  at  $120^\circ\text{C}$  showing a carbon contamination at the surface, an oxide layer of 3 nm and the nitrogen surface peak at 5 nm below the surface.

Nitrogen is probably trapped at the interface between the oxide layer and the bulk.

## 5. Conclusions

The aim of this work was attained by showing the formation of iron nitride phases by nitrogen implantation into pure iron and the dependence of these phases vs. temperature and dose. Nitrogen diffuses towards the surface during implantation and this phenomenon is enhanced with increasing temperature of the implanted specimen. The surface peak is due to trapping of nitrogen into precipitation sites located at the interface between the oxide layer and the iron in the bulk. NRA and SIMS depth distributions are in good agreement and the Mössbauer analysis shows only iron nitride formation.

## Acknowledgments

The authors are indebted to C. Poleunis for technical assistance. The research results of the

Belgian program on interuniversity attraction poles initiated by Belgian State (Prime Minister's Office) Science Policy Programming are presented in this paper. Scientific responsibility is assumed by the present authors.

## References

- 1 F. Bodart, G. Terwagne and M. Piette, *Mater. Sci. Eng.*, *90* (1987) 111-117.
- 2 N. Moncoffre, *Mater. Sci. Eng.*, *90* (1987) 99-109.
- 3 E. Ramous, G. Principi, L. Giordan, S. Lo Russo and C. Tossello, *Thin Solid Films*, *102* (1983) 97-106.
- 4 G. Terwagne, M. Piette and F. Bodart, *Nucl. Instrum. Methods B*, *19-20* (1987) 145-149.
- 5 G. Longworth and N. E. W. Hartley, *Thin Solid Films*, *48* (1978) 95-104.
- 6 J. J. Spijkerman, J. C. Travis, P. A. Pella and J. R. De Voe, *NBS Tech. Note 541*, 1971 (U.S. National Bureau of Standards).
- 7 W. Möller and E. Eckstein, *Nucl. Instrum. Methods B*, *2* (1984) 814.
- 8 N. Moncoffre, G. Hollinger, H. Jaffrezic, G. Marest and J. Tousset, *Nucl. Instrum. Methods B*, *7-8* (1985) 177-183.
- 9 M. Chabanel, C. Janot and J. P. Motte, *C.R. Acad. Sci., Ser. B*, *266* (1968) 419-422.
- 10 K. H. Eickel and W. Pitsch, *Phys. Status Solidi*, *39* (1970) 121-129.
- 11 A. J. Nozik, J. C. Wood, Jr., and G. Haacke, *Solid State Commun.*, *7* (1969) 1677-1679.
- 12 M. Piette, G. Terwagne, W. Möller and F. Bodart, *Mater. Sci. Eng.*, *B2* (1989) 189-194.